Interplay of resonant and l-window background amplitudes in $^{16}O + ^{16}O$

M. Gai, S. K. Korotky,* J. M. Manoyan, E. C. Schloemer,†
B. Shivakumar,‡ S. M. Sterbenz, S. J. Willett,§ and D. A. Bromley
A. W. Wright Nuclear Structure Laboratory, Yale University, New Haven, Connecticut 06511

H. Voit
A. W. Wright Nuclear Structure Laboratory, Yale University, New Haven, Connecticut 06511
and Physikalisches Institut der Universität Erlangen-Nürnberg, Erlangen, Federal Republic of Germany
(Received 12 July 1984; revised manuscript received 14 January 1985)

High resolution study of the $^{16}O + ^{16}O$ system at $15.5 \leq E_{c.m.} \leq 17.0$ MeV is reported including excitation functions for elastic scattering, and angle integrated cross sections for α_0 and α_1 exit channels and several γ-ray channels. All show correlated resonant structure. Fifteen angular distributions for the α_0 and α_1 exit channels are measured in $\Delta E_{c.m.} \simeq 50$ keV steps for $15.5 \leq E_{c.m.} \leq 16.4$ MeV in the angular range $17° \leq \theta_{c.m.} \leq 93°$ in steps of $\Delta\theta_{c.m.} \simeq 2.5°$. Phase shift analysis of the α_0 angular distribution was carried out. Ambiguities in the extraction of the S matrix elements are removed using the usual techniques with an additional new constraint—the measurement of cross section at selected angles (zeros of P_l) arising from a single partial wave. Reaction amplitudes corresponding to a narrow l window around the grazing partial wave are shown to dominate the cross section around $\theta_{c.m.} = 90°$. The grazing partial wave shows broad nonresonant structure; a specific parametrization of the energy dependence of the nonresonant (background) cross section corresponding to the l window is presented. The interplay of background amplitudes (l window) and resonant amplitudes is emphasized. Resonances in the α_0 channel are located at $E_{c.m.} = 15.8$, 15.9, and 16.1 MeV having $J^\pi = 10^+$, 8^+, and 8^+, respectively, and intermediate widths ($\Gamma \sim 70$ keV). Spin assignments are obtained via a phase shift analysis and study of excitation functions measured at zeros of Legendre polynomials. Parametrization of the resonance plus background cross section yields the result $\sqrt{\Gamma_0 \Gamma_\alpha}/\Gamma \simeq 1.0\%$. The extracted partial widths are analyzed in terms of the Wigner limit and suggest resonances not of dinuclear structure, but of more complicated structure. Such states, having $J^\pi = 8^+$, are found to appear systematically at the empirically determined energies: $E_{c.m.} = 4 \times 2.8 + N \times 2.4$ MeV ($N = 0, 1, 2, \ldots$) in many different heavy ion resonant systems; this may suggest that the underlying alpha particle structure of the participant nuclei may play an explicit role in these resonances.

I. INTRODUCTION

In the earliest measurements[1] on resonance phenomena in heavy ion interactions it was already clear that the $^{12}C + ^{12}C$ and $^{16}O + ^{16}O$ systems displayed strikingly different behavior. Subsequent studies delineated some 38 resonances in, and above, the barrier in $^{12}C + ^{12}C$ while none had been reported previously for the $^{16}O + ^{16}O$ system. Recently reported[2] systematics of resonance occurrence in a number of heavy ion systems involving $A = 4n$ nuclei have suggested the possibility that two quite distinct types of resonant structure are involved in the interactions of these light nuclei. In one case the interacting nuclei retain their identity to yield a binary molecular state; such dinuclear states were indeed suggested in the $^{12}C + ^{12}C$ system[3] in the Coulomb barrier region. Such states yield rich spectra[4] of vibration rotation character. Studies[5–7] on possible resonant structure in the vicinity of the Coulomb barrier in $^{16}O + ^{16}O$ indicate that a comparably rich structure of dinuclear molecular states as in the $^{12}C + ^{12}C$ case[3] does not exist. In the second case it has been suggested[2] that the molecular states are not of dinuclear character but rather involve the underlying (perhaps alpha particle) structure of each participant nucleus and are thus polynuclear in character.

The complex resonant structure observed in heavy ion scattering has eluded detailed understanding for more than two decades. It now appears plausible, however, to assume that the structure is not of one particular character, but rather that different structures of different characteristics (e.g., width) may appear embedded in one another, and that different physical phenomena dominate the scattering interaction in different energy regimes. In particular, it has been suggested that the typical heavy ion scattering excitation function can be empirically segmented into at least three regions.[8]

Region A extends up to the Coulomb barrier, and includes narrow structures of dinuclear character as in the $^{12}C + ^{12}C$ case.[3,4] Region B extends to center of mass energies several times (~ 4) the Coulomb barrier; in this region the cross section is dominated by broad structures on which are superimposed structures of intermediate width. The broad structures are thought to be characteristic of nonresonant potential scattering, and each structure in this region is characterized by the grazing partial wave appropriate to that energy. The intermediate width struc-

ture has been interpreted in terms of a double resonance mechanism involving inelastic excitation of one or both of the participants.[9] As more detailed measurements have become available it has also been found that some of this superimposed intermediate width structure appears to obey empirical systematics,[2,5,8] and the suggestion was that it may be polynuclear in character. Regions A and B are typically separated by a pronounced decrease (~ 10) in the average cross section.

Region C extends upward in energy from ~ 4 times the Coulomb barrier; it includes mainly nonresonant very broad oscillations not associated with any one particular partial wave. Again regions B and C appear to be separated by a pronounced drop (~ 10) of the average of the oscillatory cross section. In some heavy ion systems it has been suggested[8] that the drop in the average cross section (at the limit between regions B and C) occurs at the same energy where the total fusion data[10] saturate as seen on a $1/E$ plot. More recently[11] the interplay of mechanisms of different character such as width was studied for $^{16}O+^{16}O$ in a similar fashion.

Many nonresonant mechanisms have been shown to produce broad resonance-like structure. In general such (direct) reaction mechanisms are associated with amplitudes arising from a narrow window centering on the grazing partial wave. Recently, it was suggested that even within statistical models[12,13] the energy averaged partial cross sections are significantly large only within such a narrow window. Clearly such a narrow window in angular momentum, inherent in a surface interaction, could give rise to an energy dependence of the nonresonant background, and can lead to angular distribution resembling the square of a single Legendre polynomial. In consequence these nonresonant mechanisms can lead to data having all the overt characteristics of a resonance. On the other hand, the existence of such an l window reduces the number of active partial waves, and thus the partial wave decomposition of our data is, in principle, simpler.

Unambiguous physical S matrices extracted from heavy ion reaction data are an essential component of any detailed understanding of the underlying reaction mechanism. Resonance partial widths are equally important for understanding the structure of the resonant states. A comprehensive discussion of these topics may be found in Refs. 8 and 14.

We have undertaken a detailed examination of the $^{16}O+^{16}O$ system to study structures of intermediate width occurring in region B of Ref. 8 via the $^{16}O(^{16}O,\alpha_0)^{28}Si$ channel and have located resonances at $E_{c.m.}=15.8$, 15.9, and 16.1 MeV. In order to establish some of the parameters of these resonances we have carried out detailed angular distribution measurements in the resonance energy region, and have measured the $^{16}O+^{16}O$ elastic scattering function, as well as the $^{16}O(^{16}O,\alpha_1)^{28}Si^*$ cross section and $^{16}O(^{16}O,x\gamma)X$ gamma ray yields. Detailed analyses of all these data have yielded unambiguous S-matrix elements for the reaction $^{16}O(^{16}O,\alpha_0)^{28}Si$ in the resonance region. We have been able to disentangle the resonant and background amplitudes as well as examine the energy dependence of the background. From this analysis we have made the assignments $J^\pi=10^+$, 8^+, and 8^+ to the resonances at $E_{c.m.}=15.8$, 15.9, and 16.1 MeV, respectively. We have also demonstrated that the background comes from a narrow angular momentum window centered on the $l=10$ grazing[15] partial wave. The cross section at 90° is shown to be governed by this background l-window amplitude.

Finally, we note that the 8^+ resonances that we report here extend the systematic behavior that we previously reported[2] for certain resonances (in region B; see Ref. 8) in interactions between $A=4n$ nuclei. All these resonances appear to be of similar structure, other than dinuclear, and apparently involving the underlying (alpha particle cluster) structure of the participant nuclei.

II. EXPERIMENTAL ARRANGEMENT

Three different experiments were carried out utilizing ^{16}O beams from the Yale MP1 accelerator. Elastic scattering excitation functions were measured at selected angles. Angular distributions for the α_0 and α_1 exit channels were measured as were gamma ray yields from reaction products. The elastic scattering data were collected with a 15 $\mu g/cm^2$ SiO_2 target with a gold 5 $\mu g/cm^2$ flash added for normalization purposes as well as to prevent destruction of the target by electrostatic forces developed in the insulating target material itself. Elastic scattering events were identified via a kinematical coincidence. Data were taken in $\Delta E_{c.m.}=50$ keV steps at $\theta_{c.m.}=90°\pm 2°$ and $82°\pm 2°$; the latter angular range includes zeros of Legendre polynomials of the order $l=8$, 10, and 12. Absolute elastic cross sections were obtained by normalizing the data to previous results[16,17] which extend to energies well below the Coulomb barrier where the cross section is known to be that which is pure Mott in character.

The $^{16}O(^{16}O,\alpha)^{28}Si$ data were measured with a 30 $\mu g/cm^2$ WO_3 target evaporated onto 200 $\mu g/cm^2$ Au foil. Extra attention was given to evaporating the WO_3 from aluminum oxide boats in order to reduce the WO and WO_2 content of the target. Our data are consistent with previous data[18,19] also measured with a WO_3 target as well as with more recent data[20] measured with a SiO_2 target. Alpha particles produced in the reaction were detected in a sixteen-segment position-sensitive solid state detector placed 9 cm from the target. The detector subtended $\Delta\theta_{lab}\approx 31°$. Two angular settings were used to measure the complete alpha particle angular distributions. A nickel foil, of areal density 11 mg/cm^2, was used to stop all heavy reaction products. The depletion layer of the position sensitive detector (PSD) was chosen to minimize energy loss of hydrogen isotopes. In Fig. 1 we show a typical E vs X PSD spectrum. The 16 slices are evident and the energy resolution is clearly sufficient to separate α_0 from α_1 events. We note that a kinematical correction was added (via software) to these data to present loci of equal excitation energy which are parallel to the x axis and yield better position resolution. A gate was set on particular alpha particle groups to allow for projection on the X axis; a typical projection of an α_0 gate is shown in Fig. 2 for an angular distribution measured on resonance. The projected spectra were corrected for solid angle, nor-

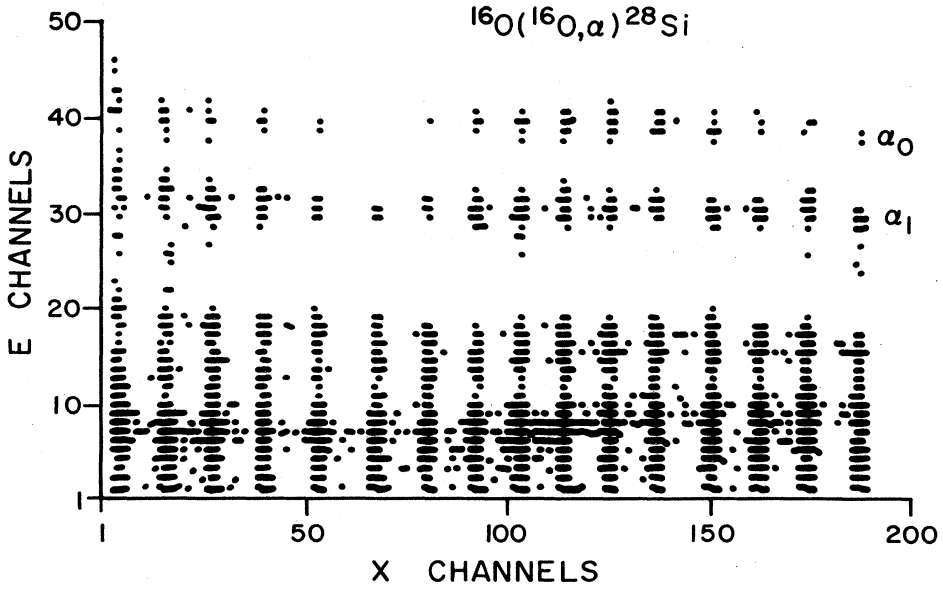

FIG. 1. Typical energy versus position two-dimensional histogram, with kinematic corrections, for the sixteen-segment position sensitive detector.

malized, and transferred to the center of mass to produce the final angular distributions. As is shown in Fig. 2, even prior to these corrections, the raw data histogram resembles a single Legendre polynomial squared (P_8^2). In this way angular distributions were measured essentially on line. Fifteen α_0 and α_1 angular distributions were measured in the range $15.5 \leq E_{\text{c.m.}} \leq 16.4$ MeV in 50 keV steps, over the angular range $17° \leq \theta_{\text{c.m.}} \leq 93°$ in $\delta\theta_{\text{c.m.}} \approx 2.5°$ steps. Typical α_0 spectrum data, as shown in Fig. 2, were collected over periods of 3—4 h with a 200 charge nA ^{16}O beam. The typical PSD count rate was 3—4 KHz, with dead time of the order of 10%. The PSD counter was cooled to $-25\,°C$ to reduce leakage current ($\sim 0.5\ \mu A$). A cold finger LN_2 trap surrounded the target to minimize carbon contaminant buildup. Typical operational vacuum was 4×10^{-7} Torr.

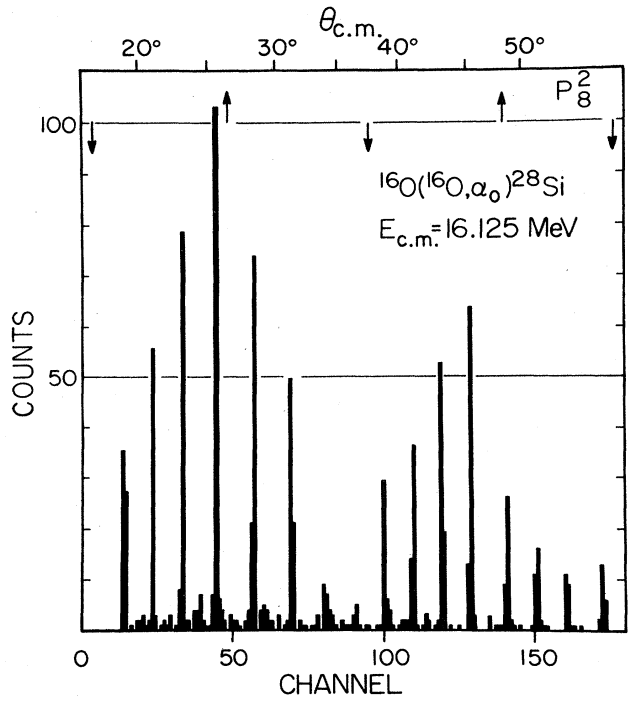

FIG. 2. A typical projection of a gate including only α_0 events, as shown in Fig. 1. The extrema of P_8^2 are shown by vertical arrows. The raw data already resemble a single Legendre polynomial squared, P_8^2.

The gamma ray yield data were measured with a 30 $\mu g/cm^2$ WO_3 target evaporated onto a 7 mg/cm^2 Au foil. The Au foil was used to slow down residual nuclei to minimize the Doppler shift of reaction product gamma rays. The gamma rays were detected in a 12% Ge(Li) detector placed at 90°, 5 cm away from the target. A typical Ge(Li) spectrum is shown in Fig. 3.

III. EXPERIMENTAL RESULTS

The results of the excitation function measurements are shown in Fig. 4. The elastic scattering differential cross section is shown at two angles as well as the angle integrated cross section for the α_0 and α_1 exit channels; the integration interval is indicated. The cross section for the α_0 and α_1 in the vicinity of $\theta_{\text{c.m.}} = 90°$ is also given. The gamma ray yield, shown in Fig. 5, also shows similar structures. These structures have also been seen in the total reaction cross section deduced from elastic scattering measurements carried out at Erlangen.[7] We note that structures appear in some cases to be shifted, with an energy shift smaller than their measured width. It bears emphasizing, however, that such correlations are neither necessary nor do they prove the existence of resonances as such; therefore, in this paper we do not make an attempt to deduce the existence of resonances through their correlated behavior, but rather through examining the nuclear

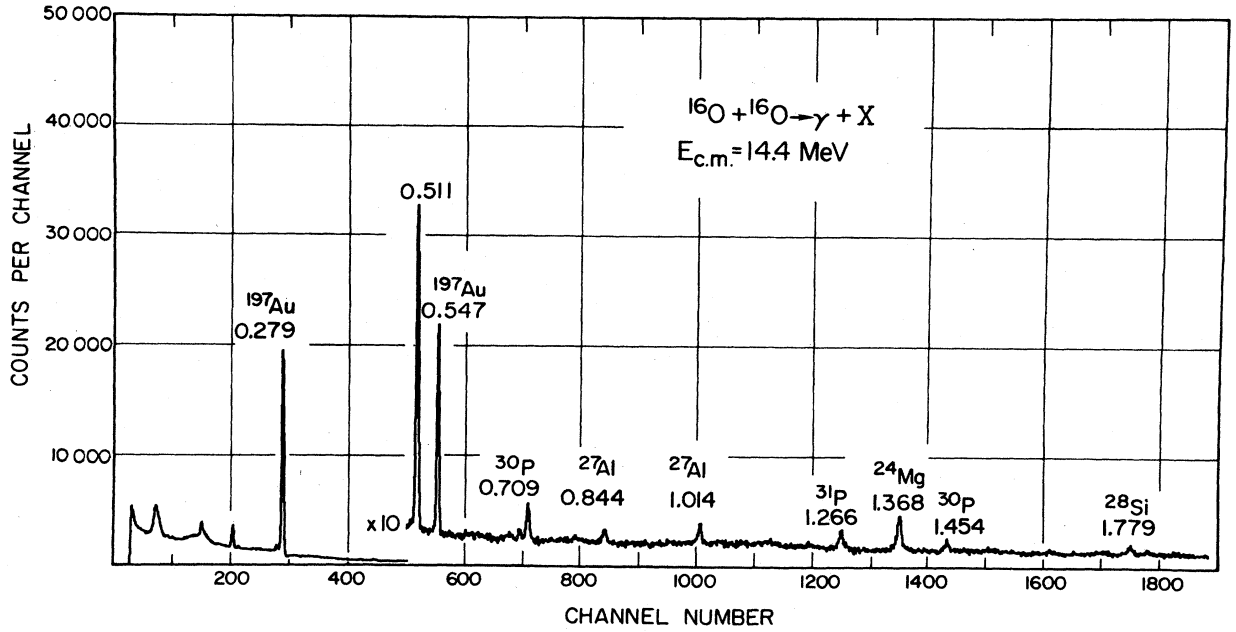

FIG. 3. A typical Ge(Li) gamma ray spectrum. The important channels are identified with respect to the residual nuclei involved.

phase shift. However, as pointed out in Refs. 20 and 44, where a correlation function study is presented, *a priori* it appears improbable that these structures represent only statistical fluctuations, since most data considered here represent angle integrated total cross sections; e.g., the α_0 data are integrated over an interval $\Delta\theta \geq 40°$, which is substantially larger than the coherence angle.[12]

Two additional important qualitative observations are

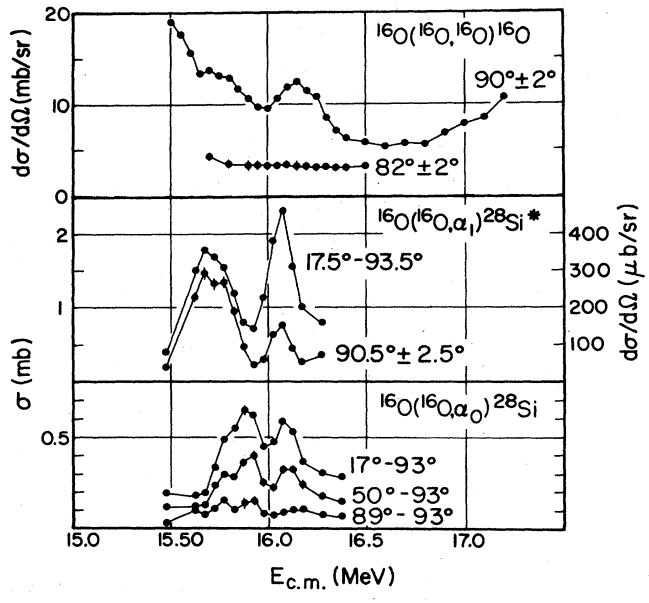

FIG. 4. Excitation functions for selected channels in the $^{16}O+^{16}O$ measured in 50 keV steps. The integration intervals for the α_0 and α_1 channels are given. The structureless elastic scattering excitation function measured at 82°, including angles for which $P_8 = P_{10} = P_{12} = 0$, should be noted, in particular.

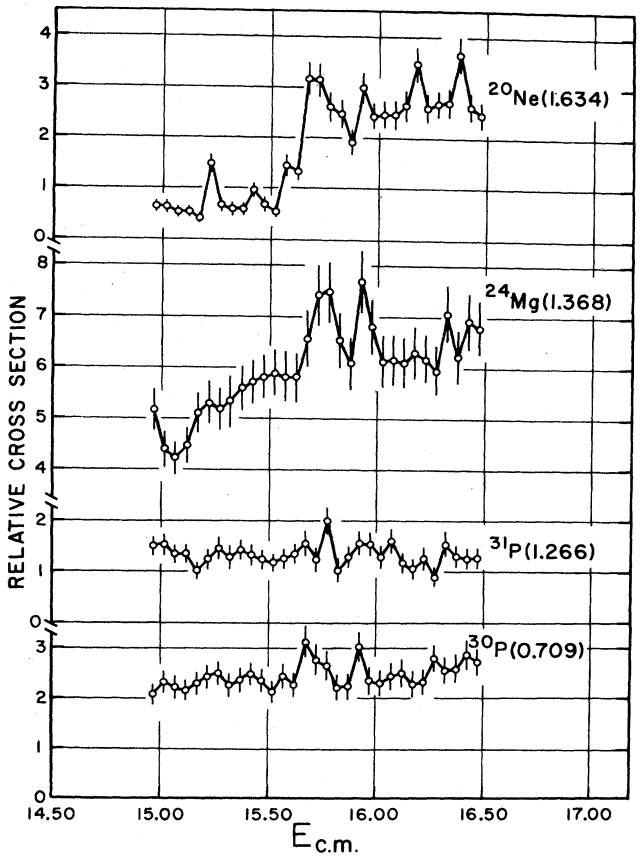

FIG. 5. Yield curve for selected gamma radiation emitted from the $^{16}O+^{16}O$ system. The residual nucleus is identified by its characteristic gamma radiation. A similar excitation function is observed for the total reaction cross section (Ref. 7).

in order concerning the elastic and α_0 excitation functions. First, the elastic data measured at 82°±2°, including zeros of P_8, P_{10}, and p_{12}, show no energy dependence, as would be expected if the structures in the elastic channel arose from any of the $l=8$, 10, or 12 partial waves. The structure in the elastic channel thus appears to arise from amplitudes within a narrow angular momentum window about $l-\text{grazing}=10$. Second, we note that the angle integrated α_0 data show structures with a 3.5 maximum to minimum ratio; at 90° we find a smaller value of 2 for this ratio. This suggests the presence of substantial background contribution to the 90° cross section.

In Fig. 6 we show 9 of the 15 measured α_0 angular distributions, together with their phase shift analysis as dis-

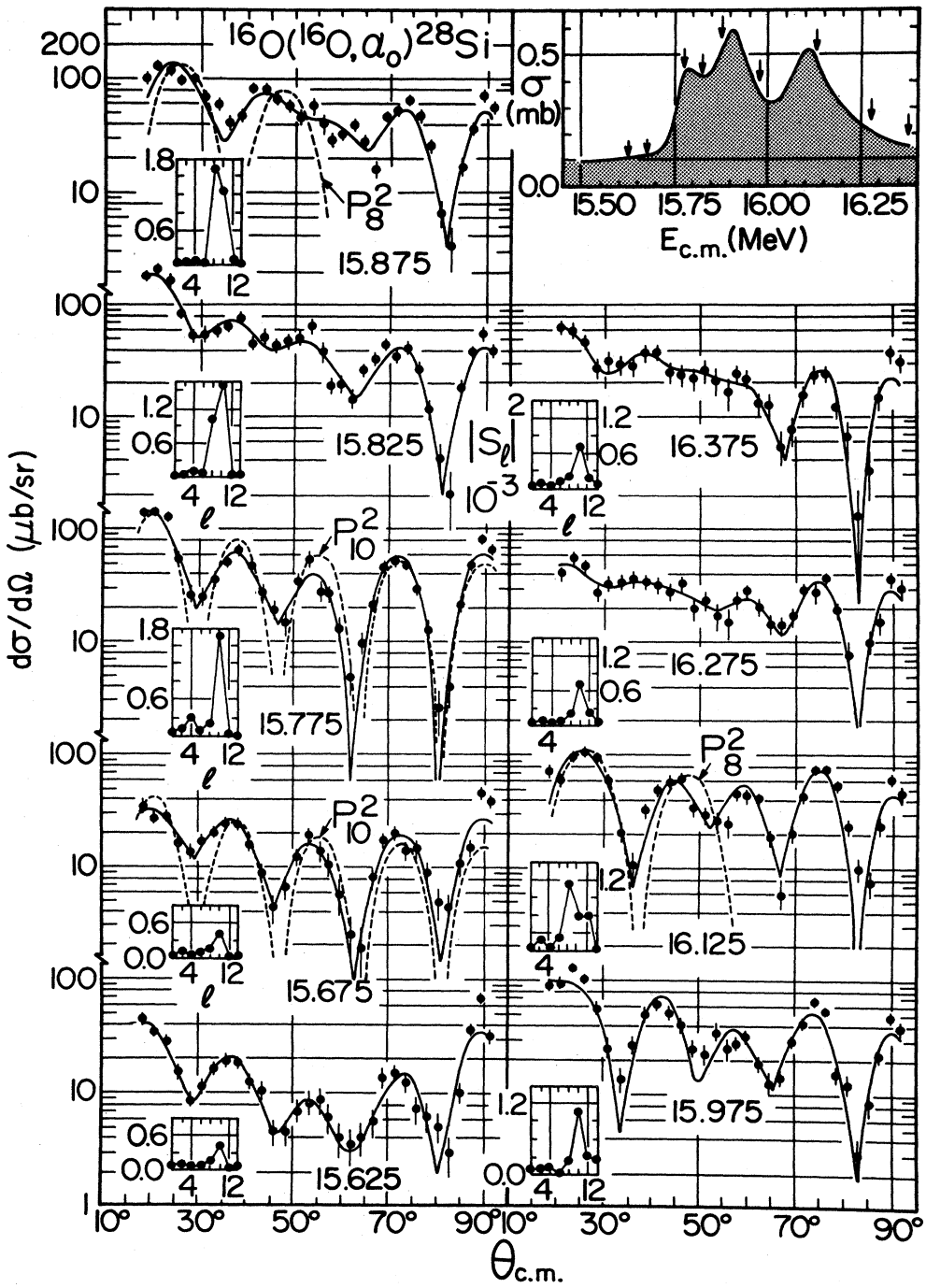

FIG. 6. Nine of the fifteen angular distributions measured for $^{16}O+^{16}O$ around $E_{c.m.}\simeq 16.0$ MeV. The total angle integrated cross section is shown in the shaded area in the insert. The arrows indicate the center of mass energies at which the angular distributions were measured. For each angular distribution we show, in the inserts, the extracted $|S_l|^2$ and the fit obtained with Eq. (1). A narrow l window around the $l=10$ grazing partial wave is observed in addition to resonances in the $l=10$, 8, and 8 partial waves.

cussed in the following section. Several observations follow from examination of the qualitative features of these data. Distributions measured off resonance (e.g., at 15.625 and 15.675 MeV) show pronounced oscillatory structure that in itself can be quite well reproduced with the square of a single Legendre polynomial P_{10}^2. However, as shown in Fig. 6, the envelope of that oscillatory pattern is maximized at 90°, unlike that of any single Legendre polynomial. We conclude then, that the cross sections measured in the minima of the α_0 excitation functions cannot arise from a single partial wave even though the angular distribution of these energies resembles a P_{10}^2, although that resemblance may suggest that only a few partial waves (and only even ones) contribute. The qualitative features of the data suggest that at the minima of the excitation function the cross section (background) is governed by contributions from a narrow angular momentum window around the $l=10$ grazing partial wave. The more quantitative phase shift analysis, to be presented in the following section, indeed, requires such a window.

The angular oscillatory pattern observed in the vicinity of 90° is almost constant over the energy region studied. The maximum and minimum at approximately 73° and 81°, respectively, persist throughout the data, as shown in Fig. 6. In the more forward angle region, no equivalent constancy is found. For example, at $\theta_{\text{c.m.}}=30°$ a maximum is observed in the angular distribution measured at $E_{\text{c.m.}}=16.125$ MeV and a minimum in those at $E_{\text{c.m.}}=15.775$ and 15.675 MeV. Again the suggestion is that slowly varying amplitudes govern the 90° data, while more rapidly varying ones determine the more forward angle data. At the maxima of the excitation function, at $E_{\text{c.m.}}=15.8$, 15.9, and 16.1 MeV, respectively, the angular distributions in the angular range $17° \leq \theta_{\text{c.m.}} \leq 50°$ resemble P_{10}^2, P_8^2, and P_8^2, respectively, as shown in Fig. 6. These considerations suggest that there are two primary contributions to the α_0 angular distribution. One arises from a narrow l window and varies slowly in energy while a second has a more pronounced energy dependence and can, in principle, be associated with energies near the maxima of the excitation function with a single partial wave ($l=10$, 8, and 8, respectively). We then observe energy dependent interference of the two contributions in the angular range $50° \leq \theta_{\text{c.m.}} \leq 70°$, as is evident in Fig. 6.

IV. DATA ANALYSIS

A. Phase shift analysis

We turn now to a more detailed quantitative analysis of our data. The fifteen α_0 angular distributions were fitted with the expression

$$\frac{d\sigma}{d\Omega}=\frac{1}{2k^2}\left|\sum_{l=0}^{14}(2l+1)\exp[i(\sigma_i+\sigma_0+2\delta_l)]S_lP_l(\theta)\right|^2 = \left|\sum A_lP_l\right|^2, \quad (1)$$

where σ_i and σ_0 are the incident and exit channel Coulomb phases and δ_l and S_l are real numbers representing the nuclear S matrix, k is the wave number in the incoming channel, and A_l is a complex number. Since the incoming channel is composed of identical bosons, it immediately follows that only Legendre polynomials of even order are included in the summation.

A typical data point at the maxima of the angular distributions was measured with ~5% accuracy. Over each narrow structure in the excitation function we collected between four and eight angular distributions, and each angular distribution contained 32 data points. Since the fits with Eq. (1) require eight different partial waves, we thus have adequate data to allow us to extract the reaction S-matrix elements.

Quite independent of the data quality, extraction of S-matrix elements is plagued by mathematical ambiguities that can be summarized as follows: For the set of 8 complex numbers $\{A_l\}_{l=0}^{l=14}$ (l=even) with 15 independently determined real numbers that correspond to a solution of Eq. (1) there exist many ($2^7=128$) other sets of complex numbers A_l' such that

$$\left|\sum A_lP_l\right|^2=\left|\sum A_l'P_l\right|^2 .$$

However, only one solution corresponds to the unique physical one. Wheeler discussed the origin of these ambiguities[21] and presented conditions required to reduce the number of ambiguities and, in principle, reveal the physical solution. Many other authors have discussed these ambiguities[22–26] more recently, classified them, and suggested algorithms for extracting nonambiguous results.

The most general procedure to resolve ambiguities involves adding physical constraints, and allows extraction of the physical solution for the S matrix. These constraints can be chosen as follows:

The angular momentum model space is limited (by physical considerations). For our reaction data the amplitudes of significance are those within a window in angular momentum space.

For reaction data we also require that the extracted A_l coefficients fit the total angle integrated cross section, i.e., we require that

$$\sigma_{\alpha_0}=2\sum\frac{|A_l|^2}{2l+1} . \quad (2)$$

For scattering data an equivalent condition holds and is usually used[22] to constrain the extraction of partial wave amplitudes. In the case discussed here clearly Eq. (2) is derived by integrating Eq. (1) and cannot be used to constrain the partial wave analysis; however, condition (2) increases the sensitivity of the fit to the dominant partial waves and thus is helpful in the search procedure.

When the physical $|S_l|^2$ are known, we require the fit using Eq. (1) to reproduce them. For example, if (as in our case) only the $l=8$, 10, and 12 partial waves contribute significantly, we may choose an angle for which $P_8 \approx P_{12} \approx 0$ and $P_{10} \equiv \max$ and thus directly measure $|S_{10}|^2$. As we shall show, such a condition can be applied to our data, and it is the most severe requirement that we impose on the extraction of the S-matrix element. Physically it directly reflects the surface nature of heavy ion interactions.

A χ^2 search on the parameter space of Eq. (1) was per-

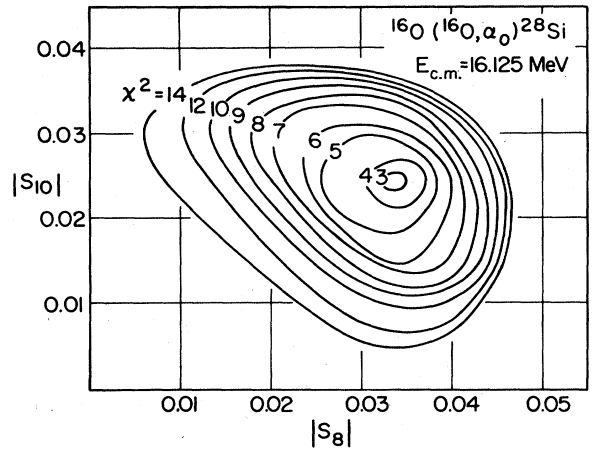

FIG. 7. A χ^2 contour plot for the angular distribution measured on resonance, at $E_{c.m.}=16.125$ MeV, for the S_8 and S_{10} parameters of Eq. (1). All fits are sensitive only to the $l=8$, 10, and 12 partial waves.

formed for our data; in Fig. 7 we show typical χ^2 contours for $|S_8|$ and $|S_{10}|$. It was found that χ^2 is only sensitive to variations in the parameters S_8, S_{10}, and S_{12}, reflecting the fact that our angular distributions have a characteristic oscillatory pattern for which all other $P_l(\cos\theta)$ oscillate either too slowly or too rapidly in angle. From this we conclude that the background contributions from the $l=0$, 2, 4, 6, and 14 partial waves, while non-negligible, are small. We, therefore, performed a fit with no restrictions on the $l=8$, 10, and 12 partial waves, and varied the $l=0$, 2, 4, 6, and 14 partial waves below an upper limit $S_l \leq 0.02$. This typically yields a contribution of these partial waves to the total reaction cross section which is about an order of magnitude smaller than the contributions of the $l=8$, 10, and 12 partial waves. Because of the statistical nature of the background we did not, however, require it to be either smoothly varying or to have any fixed value. The fit using Eq. (1) can thus be considered to be a fit using three partial waves plus background. While the fit by itself could be affected by the background contributions, and thus could, in principle, alter our spin assignment, we emphasize that the additional restrictions—the most important one being the study of the cross section at zeros of Legendre polynomials—allow us to assign spins. For all partial waves initial guesses based on random numbers were used. With these conditions the data were fitted and a single well-defined deep minimum in χ^2 was found with $\chi^2 \leq 3$, as shown in Fig. 7. Nine typical fits, thus obtained, are shown in Fig. 6 together with the extracted $|S_l|^2$ parameters for $l=0,2,4,\ldots,14$. As shown in the inset of Fig. 6, a quite acceptable reproduction of the angle integrated cross section for the α_0 exit channel is achieved. Furthermore, we find that the angle integrated cross section is almost entirely determined by contributions from the $l=8$, 10, and 12 partial waves.

Since only these three partial waves contribute at $\theta \simeq 37.5°$, a zero of P_8, near a zero of P_{12}, and a maximum of P_{10}, the cross section is essentially given by $|S_{10}|^2$. We thus require our extracted S_{10} parameter to fit the cross section measured at $\theta_{c.m.} \simeq 37.5°$. As shown in Fig. 8, an acceptable fit is obtained. Such a requirement on our extracted S-matrix element resolves the ambiguities. At $\theta \simeq 30°$, a zero of P_{10}, only the $l=8$ partial wave and a constant background, which reflects the small contribution from many other partial waves, are required. At $\theta \simeq 25°$, a zero of P_{12}, the $l=8$ and $l=10$ partial waves both contribute and reproduce the observed structures.

B. Resonance parametrization

Narrow resonances in the $l=8$ partial wave at $E_{c.m.}=15.9$ and 16.1 MeV, and in the $l=10$ partial wave at $E_{c.m.}=15.8$ MeV, are evident in the extracted S-matrix elements shown in Fig. 8. In addition, however, we note that a resonance in the l_0 partial wave, $J=l_0$, cannot appear at an angle for which $P_{l_0}=0$. With the observation that only the $l=8$, 10, and 12 are important here, measurements at $\theta=37.5°$ (a zero of P_8), $\theta=30°$ (a zero of P_{10}), and $\theta=25°$ (a zero of P_{12}) allow us, by way of elimination, to confirm the assignments of $J^\pi=10^+$, 8^+, and 8^+ to the resonances at $E_{c.m.}=15.8$, 15.9, and 16.1 MeV, respectively, as shown in Fig. 8.

The extracted S-matrix elements shown in Fig. 8 were fitted with a smooth background plus resonance term:

$$\begin{aligned} S_l^{\text{tot}} &= S_l e^{2i\delta_l} \\ &= \bar{S}_l^{\text{bg}} + \bar{S}_l^{\text{res}} \\ &= S_l^{\text{bg}} e^{2i\delta_l^{\text{bg}}} + e^{2i(\phi+\delta_l^{\text{bg}})} \frac{i\sqrt{\Gamma_0\Gamma_\alpha}}{E-E_R+i\Gamma/2}\delta_{l,l_R} . \end{aligned} \tag{3}$$

The resonant parameters are shown in Table I. The decomposition [Eq. (3)] of the total S matrix element shown in Fig. 8 supports the existence of sharp resonances with $J^\pi=10^+$, 8^+, and 8^+ at $E_{c.m.}=15.8$, 15.9, and 16.1 MeV, respectively, each interfering with a smooth background. The calculated S matrices are plotted in a Cauchy-Argand diagram[21] in Fig. 9, and show the expected resonant behavior. The extracted values of $\Gamma_0\Gamma_\alpha/\Gamma^2$

TABLE I. Resonance parameters for $^{16}O+^{16}O$.

$E^R_{c.m.}$	J^π	Γ (keV)	$\sqrt{\Gamma_0\Gamma_\alpha}/\Gamma$	S^{bg} ($E=E^R$)	Γ_0 (keV)[a]	θ_0^2 (%)[b]	Γ_α (keV)	θ_α^2 (10^{-5})[b]
15.8	10^+	70	0.01	0.03	1.8	0.2	0.3	5.0
15.9	8^+	80	0.015	0.018	2.4	0.2	0.6	8.5
16.1	8^+	60	0.01	0.018	0.9	0.06	0.4	6.0

[a]Extracted from σ_R of Ref. 7.
[b]Calculated for $R=1.5(A_1^{1/3}+A_2^{1/3})$ fm.

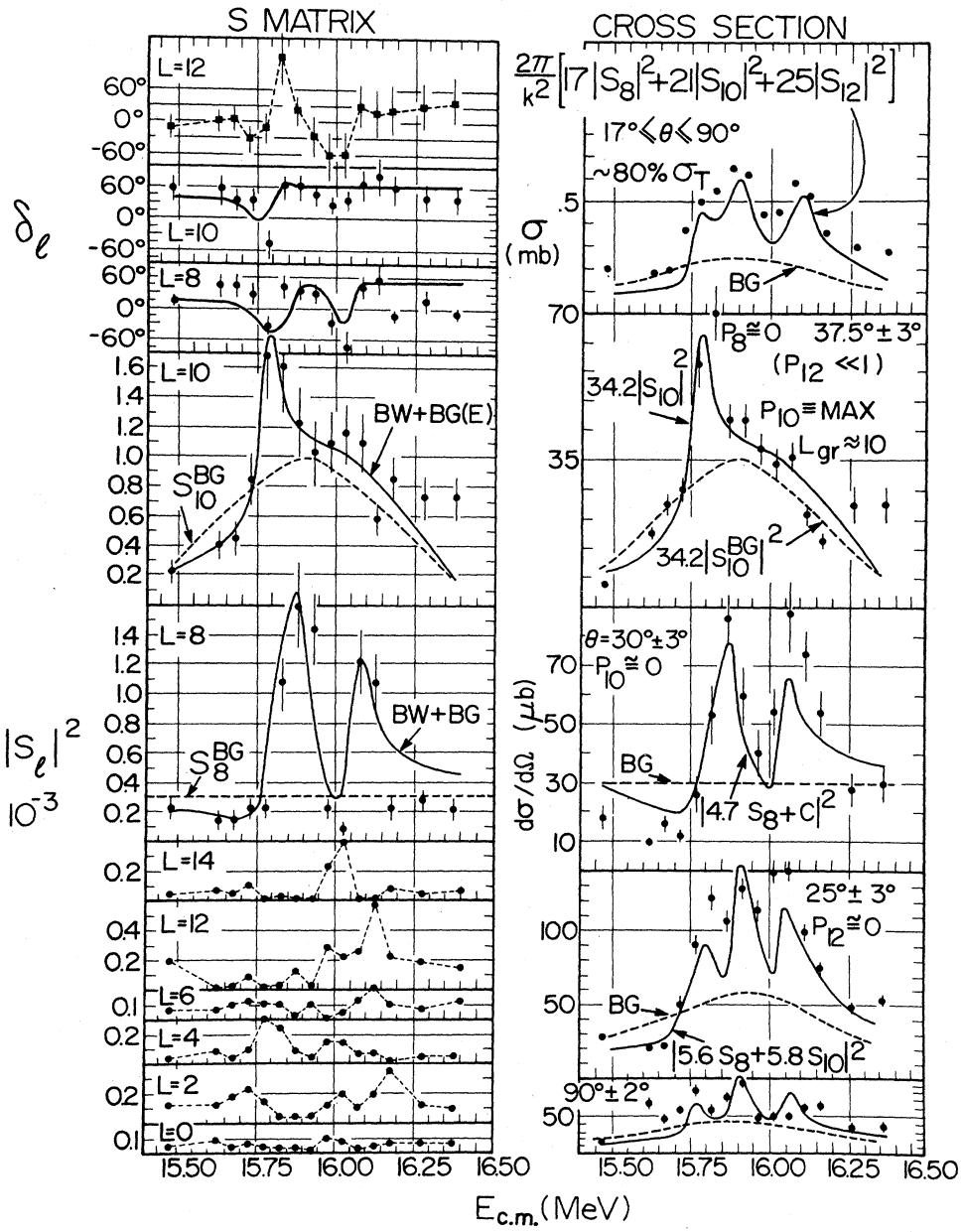

FIG. 8. The extracted S-matrix elements and measured cross sections. On the left we show by points the values of the S_l $(0\leq l\leq 14)$ and δ_l $(8\leq l\leq 12)$ parameters as extracted from fitting the angular distributions using Eq. (1). The error bars on these points are calculated using the χ^2 search as shown in Fig. 7. A Breit Wigner plus background parametrization [Eq. (3)] is shown in solid lines. The background is indicated. Note that in our original Fig. 2 of Ref. 5, a numerical error of a factor of 2 was introduced when δ_l of Eq. (3) were plotted. The actual resonance effect in δ_l should have been twice the value given in Fig. 2 of Ref. 5.

are in good agreement with the systematics of α_0 data measured in the region above the barrier in other heavy ion systems.[27–30] Since $|S^{\rm res}|$ is maximized at $2\times\sqrt{\Gamma_0\Gamma_\alpha}/\Gamma\approx 0.03$, we note that $|S^{\rm bg}|$ is non-negligible at $E\approx E_R$. The important effect of the background at 90° will be discussed below.

For the extraction of Γ_0, as listed in Table I, we used the total reaction cross section measured[7] for $^{16}O+^{16}O$ from the measured elastic channel using the sum-of-differences method which was recently carefully reexamined.[31] This cross section is given by

$$\sigma=\sigma^{\rm bg}+\sigma^{\rm res}\,,$$
$$\sigma^{\rm res}=2\frac{4\pi}{k^2}\frac{\Gamma_0(1-\Gamma_0)}{\Gamma^2}(2l+1)\,. \tag{4}$$

This quadratic equation in $\Gamma_0/\Gamma=x$ has two solutions $(x_1+x_2=1)$. With the use of the 90° elastic scattering ex-

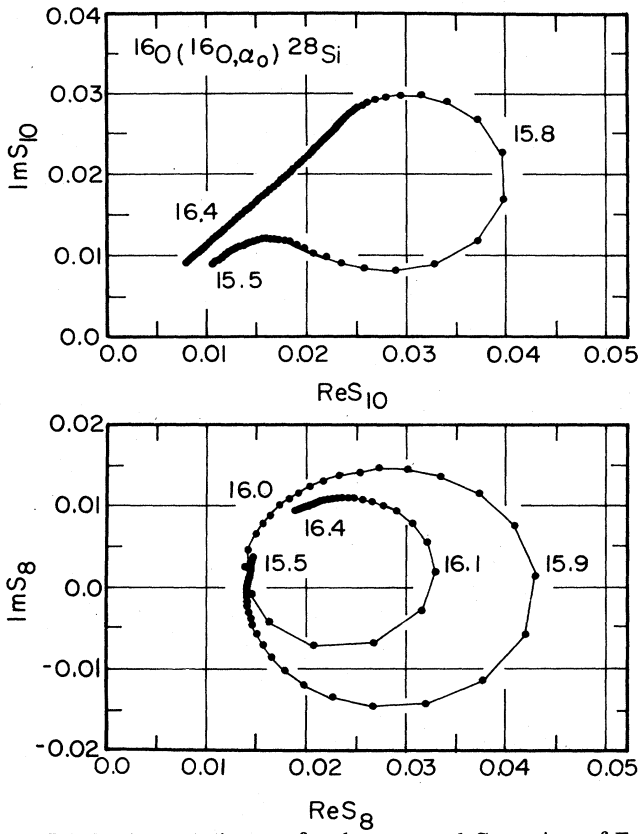

FIG. 9. Argand diagram for the extracted S matrices of Eq. (3) for the $l=8$ and $l=10$ partial waves. The diagrams were calculated using the parameters of Table I for Eq. (3) in 10 keV steps. The energies on and off resonance are given.

citation function, we obtain upper or lower bounds on $x=\Gamma_0/\Gamma$ and thus can differentiate between extreme solutions, as, for example, $x_1=10\%$ and $x_2=90\%$.

The extracted resonance partial widths are expressed as fractions (θ^2) of the Wigner limit:

$$\Gamma_i=\theta_i^2\frac{2kR}{F_l^2+G_l^2}\frac{3}{2}\frac{\hbar^2c^2}{2\mu c^2R^2}\,, \tag{5}$$

where $R=1.5(A_1^{1/3}+A_2^{1/3})$, and F_l and G_l are the regular and irregular Coulomb functions estimated at $\rho=kR$. These quantities are listed in Table I. The small fractions of the Wigner limit obtained suggest states which are not of dinuclear $^{16}O+^{16}O$ or $\alpha+^{28}Si$ structure. Since these are the dominant channels in the energy range under study, we conclude that these states are not of dinuclear structure.

C. Background parametrization

From Fig. 8, it is clear that the background parameter S_l^{bg} for the $l=10$ grazing partial wave is energy dependent. In contrast, the background parameters for the $l=8$ partial wave are constant. This energy dependence in the $l=10$ grazing partial wave may reflect potential scattering phenomena[15] in the entrance channel. Thus we chose to parametrize the S matrix as a derivative of a Fermi function, which is related to the derivative of the S matrix in the strong absorption limit:

$$S_{l=10}^{bg}\propto\frac{e^{-(E-E_0)/\Delta}}{[1+e^{-(E-E_0)/\Delta}]^2} \tag{6}$$

with E_0 and Δ as fitting parameters ($E_0=15.9$ MeV and $\Delta=0.25$ MeV). In Fig. 10 we show this parametrization of the background, together with $|S_{10}^{tot}|^2$, and the cross section measured at $\theta=37.5°$ which is proportional to

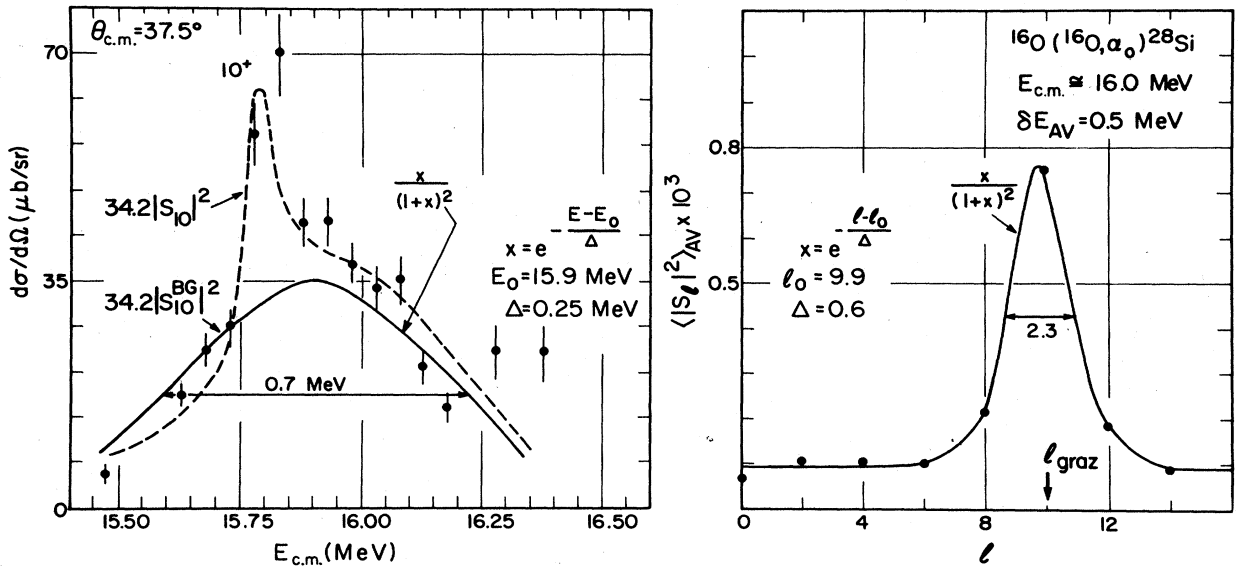

FIG. 10. Energy-averaged, background S_l matrices extracted from our data. Resonance contributions were omitted. The fit and fitting parameters are shown; they resemble the predicted l windows of Braun-Munzinger and Barrette (Ref. 12) obtained using a statistical model.

$|S_{10}^{\text{tot}}|^2$. It is clear that the broad (0.7 MeV wide) maximum centered at $E_{\text{c.m.}}=15.9$ MeV should not be attributed to a resonance effect but rather results from grazing partial wave effects. In Fig. 10 we also show the energy averaged $|S_l|^2$, averaged over all 15 data points with the resonant contribution subtracted. A well-defined window around l grazing ($=10$) is observed. We parametrize that window again as

$$\langle |S_l|^2 \rangle_{\text{av}} \propto \frac{e^{-(l-l_0)/\Delta}}{[1+e^{-(l-l_0)/\Delta}]^2} \tag{7}$$

with l_0 and Δ as fitting parameters ($l_0=9.9$ and $\Delta=0.6$). Clearly the $l=10$ partial waves dominate; however, the $l=8$ and $l=12$ contributions are only a factor of 2 smaller (a factor of 4 in S_l^2), and are clearly non-negligible. It is interesting to note that such an l window is predicted by statistical models,[12] with similar widths corresponding to a large (25°) coherence angle. A similar window has also been observed recently in our study[27] of the ^{12}C(^{16}O,α_0)^{24}Mg reaction.

V. DISCUSSION

A. The role of the grazing partial wave

The complete characterization of the S matrix, extracted from our high resolution data, indicates a substantial contribution from the nonresonant background. This background is shown to dominate the cross section in the vicinity of $\theta_{\text{c.m.}}\simeq 90°$. It follows that excitation functions measured at one angle, in particular, for symmetric systems, the extreme angle $\theta=90°$, are not sufficient to establish the existence of resonances. The energy dependence of the grazing partial wave amplitude observed here, and the narrow l window around l grazing, can, as shown here, produce resonance-like structure, with angular distributions very similar to a single Legendre polynomial squared, P_{lg}^2. In this case the scattering wave function does not necessarily concentrate at the origin, as is required for a resonance.[32] We have found similar phenomena in the ^{16}O+^{12}C system[27] where the ^{12}C(^{16}O,α_0)^{24}Mg cross section measured near $\theta_{\text{c.m.}}=180°$ was dominated by the background.

b. Possible origin of the background

We have attempted to relate the extracted parameters l_0,E_0 and Δ_E,Δ_l, discussed above, in search of an understanding of the mechanism that produces the narrow l window and the energy dependence of the cross section contribution from the grazing partial wave.

The rather small value of $\Delta_E=0.25$ MeV (FWHM=0.7 MeV) is associated with a low energy, $E_{\text{c.m.}}=16$ MeV, and is clearly energy dependent, as suggested in calculations of potential scattering.[15] On the

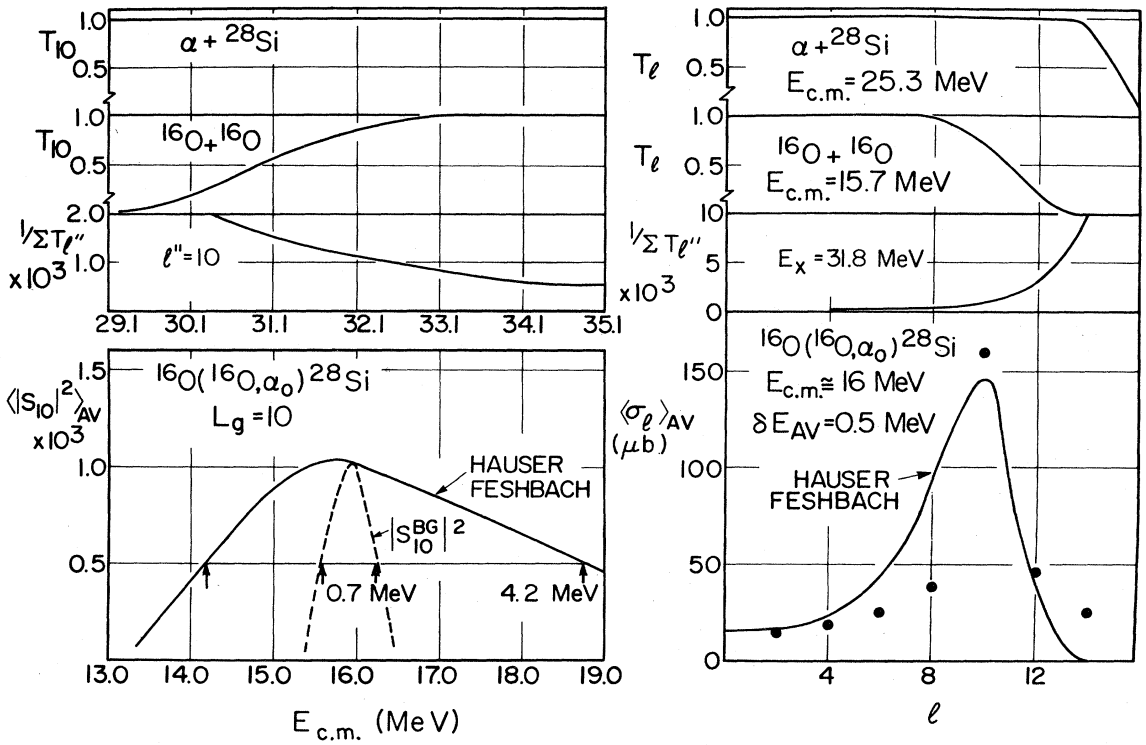

FIG. 11. Statistical model calculations of the energy averaged l window, and the energy dependence of the grazing partial wave $|S_{10}|^2$. The extracted data are shown by points, or by dashed curve. The center of mass energies and excitation energy in ^{32}S are shown.

other hand, the parameter $\Delta_l \simeq 0.7$, extracted in the present study and from our $^{12}C(^{16}O,\alpha_0)^{24}Mg$ study,[27] appears to be energy independent, and is consistent with the FWHM ($\simeq 2.5$) predictions of a statistical model.[12]

It thus appears reasonable to attempt to describe the energy averaged background l window within a Hauser-Feshbach formalism.[33] In that model the energy averaged partial cross sections are given by

$$\langle \sigma_{c,c'} \rangle_{\text{av}} = \frac{1}{k^2} \frac{T_l T_{l'}}{\Sigma T_{l''}} , \tag{8}$$

where T_l ($T_{l'}$) are the transmission coefficients in the entrance (exit) channels. In the statistical model[34] we find immediately that

$$\Sigma T_{l''} = 2\pi\Gamma\rho , \tag{9}$$

where Γ is the mean compound level width (coherence width) and ρ is the level density.

We have used the optical model[15] of Gobbi *et al.* for the $^{16}O+^{16}O$ entrance channel and the optical model[35] used similarly for alpha[35] particle scattering for the $\alpha+^{28}Si$ exit channel. As shown in Fig. 11, the small Q value (large $E_{\text{c.m.}}$) and small Coulomb barrier of the $\alpha+^{28}Si$ exit channel yield transmission coefficients very near unity, and the cross section is then only dependent upon characteristics of the incoming entrance channel. Using the level density of Ref. 34 and a reasonable coherence[18] width of $\Gamma = 100$ keV (measured at higher energies), we find that a statistical model can indeed reproduce[12] the l window observed in our study, as shown in Fig. 11. It bears emphasis that no adjustment of parameters was employed in these calculations. The width of the calculated l window appears to be somewhat larger than required, but the absolute value and the position of the maximum are well reproduced. The calculations also produce energy dependence in the grazing partial wave $|S_{10}|^2$ of width considerably larger than that observed.

C. Possible resonance origin

As already discussed, the resonances having $J^\pi = 10^+$, 8^+ and 8^+ at $E_{\text{c.m.}} = 15.8$, 15.9, and 16.1 MeV are not of dinuclear structure. It has been noted[2] that in several heavy ion systems pronounced resonance structures *appear only in the elastic channel* with no apparent corresponding structure in the inelastic channels. Some ten such structures are known in light heavy ion systems; they appear at center of mass energies given by

$$E_{\text{c.m.}} = 4\times 2.8 + N\times 2.4 \text{ MeV } (N = 0,1,2,\ldots) . \tag{10}$$

For some of these resonances the spins and parities are known and all such are found to be 8^+, even though in the different systems the grazing partial wave at the resonant energy varies between $l = 5$ and 13. Table II lists these resonances, several of which are now under study in this laboratory, and we shall publish a more detailed paper on their systematics in the near future. It appears that in some cases, such as that studied here and in the $^{16}O+^{12}C$ system[27] around 11.2 and 13.6 MeV, the 8^+ resonances are fragmented into at least two daughters, one above and one below the energy given by the empirical expression [Eq. (10)].

We have suggested that these resonances may arise from normal modes of a polynuclear molecular configuration, in which the underlying alpha particle cluster structure of the participant nuclei may play an important role. It can be shown that the energy of a number of the nor-

TABLE II. $J^\pi = 8^+$ resonance systematics.[a]

System	$E_{\text{c.m.}}$	$E_{\text{c.m.}}^{\text{empirical}}$[b]	J^π	l grazing[c]	Ref.
$^{12}C+^{12}C$	11.3	11.2	8^+	8	3
$^{16}O+^{12}C$[d]	10.8[d]	11.2	8^+	5	27
	11.7[d]	11.2	8^+	6	
	13.2[d]	13.6	8^+	8	
	13.7[d]	13.6	8^+	9	
$^{16}O+^{16}O$	11.9[e]	11.2	8^+	4	present
	15.9[d]	16.0	8^+	10	
	16.1[d]	16.0	8^+	10	
$^{16}O+^{20}Ne$[f]	18.5	18.4	(8^+)	13	36
$^{16}O+^{24}Mg$[f]	18.5	18.4	(8^+)	12	37
$^{16}O+^{28}Si$[f]	21.0	20.8	(8^+)	11	38–41
$^{12}C+^{24}Mg$[f]	13.5	13.6	(8^+)	5	42,43
	16.5	16.0		8	

[a]Except for the $^{12}C+^{12}C$ all thus far known 8^+ resonances (in all systems) are listed. In $^{12}C+^{12}C$ several more 8^+ resonances are known, but the 11.3 MeV structure is clearly pronounced and correlated in all exit channels studied thus far.

[b]As in the empirical formula, Eq. (10).

[c]Deduced from conventional optical model calculations (the l value for which $T_l = \frac{1}{2}$).

[d]Note that two 8^+ resonances are observed below and above the empirical energy.

[e]A spin multiplet of $J^\pi = 2^+,4^+,6^+,8^+$ is observed (Ref. 6) within 1 MeV.

[f]These structures are again seen only in *the elastic channel* and not in the inelastic scattering (to the first 2^+ state) even though the inelastic channel is well matched, as discussed in the text.

mal modes of any relatively simple classical system of alpha particles can be obtained by summing over effective 0^+ and 2^+ quanta that arise in the relative motion of two alpha particles. It has been noted[2] that the "2^+ quantum" at 2.8 MeV [as in Eq. (10)] is identical to the energy of the 2^+ resonant state in ^{8}Be and that the "0^+ quantum" at 2.4 MeV [as in Eq. (10)], is related to the binding energy properties of $A=4n$ alpha particle nuclei.[2] These statements are still purely empirical observations, and are under continuing study. The data thus far available, however, may begin to suggest the presence of a new family of resonances systematically related in many light heavy ion systems. The parameters which appear in Eq. (10) may suggest that this family of resonances is related to alpha particle clustering behavior in these nuclei.

VI. CONCLUSION

We have shown that in the $^{16}O+^{16}O$ system studied here, ambiguities in the phase shift analysis of resonance data can be resolved by adding additional physical constraint. We have also shown that the cross section from a single partial wave can be measured via an appropriate choice of the scattering angle.

We have found three new resonances in the $^{16}O+^{16}O$ system—a system that was thought to be resonance-free. These have $J^\pi=10^+$, 8^+, and 8^+ and occur at $E_{c.m.}=15.8$, 15.9, and 16.1 MeV, respectively. Background arising from a narrow l window centering on the grazing partial wave leads to energy dependent cross sections and to nonresonant angular distributions similar to P_l^2. At some extreme angles (e.g., $\theta_{c.m.}=90°$) the cross section has been found to include large contributions from the nonresonant energy-dependent background. The 8^+ resonances found here may be members of a new family of polynuclear resonances, having alpha particle substructure, which appear in many different light heavy ion systems.

We note that Liendo *et al.*[44] from Florida State University have published different analyses of similar data measured with high resolution for the $^{16}O(^{16}O,\alpha_0)^{20}Si$ reaction. The results of Ref. 44 are in excellent agreement with those presented here.

This work was supported by the U.S. D.O.E. under Contract No. DE-AC02-76ER03074.

*Permanent address: Bell Laboratories, Holmdel, NJ 02733.
†Present address: Lawrence Berkeley Laboratory, University of California, Berkeley, CA 94720.
‡Temporary address: Physics Division, Oak Ridge National Laboratory, Oak Ridge, TN 37830.
§Permanent address: 3M Center, St. Paul, MN 55116.

[1]D. A. Bromley, J. A. Kuehner, and E. Almqvist, Phys. Rev. Lett. **4**, 365 (1960).
[2]M. Gai, Bull. Am. Phys. Soc. **24**, 843 (1979); **25**, 592 (1980); in Proceedings of the International Conference on Nuclear Physics, Berkeley, California, Lawrence Berkeley Laboratory Report LBL-11118, 1980 (unpublished), pp. 424, 425; M. Gai and D. A. Bromley (unpublished).
[3]K. A. Erb and D. A. Bromley, Phys. Rev. C **23**, 2781 (1981).
[4]F. Iachello, Phys. Rev. C **23**, 2778 (1983).
[5]M. Gai, E. C. Schloemer, J. E. Freedman, A. C. Hayes, S. K. Korotky, J. M. Manoyan, B. Shivakumar, S. M. Sterbenz, H. Voit, S. J. Willett, and D. A. Bromley, Phys. Rev. Lett. **47**, 1878 (1981).
[6]G. Gaul, W. Bickel, W. Lahmer, and R. Santo, in *Proceedings of the International Symposium on Resonances in Heavy Ion Reactions, Bad Honeff, 1981* (Springer, Berlin, 1982), p. 72.
[7]W. Tiereth, Z. Basrak, H. Voit, N. Bischof, R. Caplar, P. Duck, H. Frolich, B. Nees, E. Nieschler, and W. Schuster, Phys. Rev. C **28**, 735 (1983).
[8]D. A. Bromley, as in Ref. 6, p. 3.
[9]W. Scheid, W. Greiner, and R. Lemmer, Phys. Rev. Lett. **25**, 176 (1970).
[10]D. G. Kovar, D. F. Geesaman, T. H. Braid, Y. Eisen, W. Henning, T. R. Ophel, M. Paul, K. E. Rehm, S. J. Sanders, P. Sperr, J. P. Schiffer, S. L. Tabor, S. Vigdor, and B. Zeidman, Phys. Rev. C **20**, 1305 (1979).
[11]K. Langanke, H. Friedrich, and S. E. Koonin, Phys. Rev. Lett. **51**, 1231 (1983).
[12]P. Braun-Munzinger and J. Barrette, Phys. Rev. Lett. **44**, 719 (1980).
[13]M. S. Hussein and A. Szanto De Toledo, Phys. Lett. **107B**, 173 (1981).
[14]P. Braun-Munzinger, Nucl. Phys. **A409**, 31c (1983); P. Braun-Munzinger and J. Barrette, Phys. Rev. **87**, 209 (1982).
[15]A. Gobbi, R. Wiland, L. Chua, D. Shapira, and D. A. Bromley, Phys. Rev. C **7**, 30 (1973).
[16]J. V. Maher, M. W. Sachs, R. H. Siemssen, A. Weidinger, and D. A. Bromley, Phys. Rev. **188**, 1665 (1969).
[17]H. Spinka and H. Winkler, Nucl. Phys. **A233**, 456 (1974).
[18]R. E. Shaw, Jr., J. C. Norman, R. Vandenbosch, and J. C. Bishop, Phys. Rev. **185**, 1040 (1969).
[19]R. B. Leachman, P. Fessenden, and W. R. Gibbs, Phys. Rev. C **6**, 1240 (1972).
[20]D. Pocanic, K. Van Bibber, J. Dunham, W. A. Seale, F. Sperisen, and S. S. Hanna, Phys. Rev. C **30**, 1520 (1984).
[21]J. A. Wheeler, Phys. Rev. **59**, 16 (1941).
[22]A. C. Heenskerk, L. P. Kok, and M. DeRoo, Nucl. Phys. **A244**, 15 (1975).
[23]E. Barrelet, Nuovo Cimento **8A**, 331 (1972).
[24]P. Charles, in Proceedings of the Deusieme Colloque Franco-Japonais De Physique Nucleaire Avec Des Ions Lourds, Gif-Sur-Yvette, Commisariat A l'energie Atomique Report IN2P3, 1979, p. 87; Ph.D. thesis, Institut de Physique Nucléaire, Orsay, 1981 (unpublished), English translation, Yale internal report (unpublished).
[25]C. Marty, see Ref. 6, p. 216.
[26]A. Gersten, Nucl. Phys. **A219**, 317 (1974).
[27]E. C. Schloemer, M. Gai, J. F. Ennis, M. Ruscev, B. Shivakumar, S. M. Sterbenz, N. Tsoupas, and D. A. Bromley, Phys. Rev. Lett. **51**, 881 (1983).
[28]K. A. Erb, R. R. Betts, D. L. Hanson, M. W. Sachs, R. L. White, P. P. Tung, and D. A. Bromley, Phys. Rev. Lett. **37**, 670 (1976).
[29]W. Galster, W. Treu, P. Duck, H. Frohlich, and H. Voit, Phys. Lett. **67B**, 262 (1977).
[30]M. L. Halbert, F. E. Durham, and A. Van der Woude, Phys. Rev. **162**, 899 (1967).
[31]C. Marty, Z. Phys. A **309**, 261 (1983).

[32]J. M. Blatt and V. F. Weiskopf, *Theoretical Nuclear Physics* (Wiley, New York, 1952).
[33]H. Feshbach, *Nuclear Spectroscopy* (Academic, New York, 1960), Vol. B, p. 665.
[34]A. Richter, *Nuclear Spectroscopy and Reactions* (Academic, New York, 1974), Vol. B, Chap. IV D.1, p. 343.
[35]J. B. England, E. Casal, A. Garcia, T. Picazo, J. Aguilar, and H. M. Sen Gupta, Nucl. Phys. **A284**, 29 (1977).
[36]M. Gai, G. M. Berkowitz, P. Braun-Munzinger, C. M. Jachcinski, C. E. Ordonez, T. R. Renner, and C. D. Uhlhorn, Phys. Rev. C **30**, 925 (1984).
[37]S. M. Lee, J. C. Adloff, P. Chevallier, D. Disdier, V. Rauch, and F. Scheibling, Phys. Rev. Lett. **42**, 429 (1979).
[38]P. Braun-Munzinger, G. M. Berkowitz, M. Gai, C. M. Jachcinski, T. R. Renner, and C. D. Uhlhorn, Phys. Rev. C **24**, 1010 (1981).
[39]M. C. Mermaz, Phys. Rev. C **23**, 751 (1981).
[40]M. Gai, H. Voit, and D. A. Bromley, Yale report, 1981, p. 205 (unpublished).
[41]M. C. Mermaz, E. R. Chavez-Lomeli, J. Barrette, B. Berthier, and A. Greiner (unpublished).
[42]M. C. Mermaz, A. Greiner, B. T. Kim, M. J. Levine, E. Muller, M. Ruscev, M. Petrascu, M. Petrovici, and V. Simion, Phys. Rev. C **24**, 1512 (1981).
[43]M. C. Mermaz, M. Ruscev, M. Gai, J. F. Ennis, K. N. Gamadia, S. M. Sterbenz, N. Tsoupas, and D. A. Bromley, Nucl. Phys. **A429**, 351 (1984).
[44]J. A. Liendo, D. L. Gay, and N. R. Fletcher, Phys. Rev. C **31**, 473 (1985).